Biophysical Chemistry 140 (2009) 57–61

Contents lists available at ScienceDirect

Biophysical Chemistry

journal homepage: http://www.elsevier.com/locate/biophyschem

Raman spectroscopic investigation on the interaction of malignant hepatocytes with doxorubicin

Jianyu Guo, Weiying Cai, Bing Du, Min Qian, Zhenrong Sun *

State Key Laboratory of Precision Spectroscopy, and Department of Physics, and Department of Biology, East China Normal University, Shanghai 200062, PR China

ARTICLE INFO

Article history:
Received 12 September 2008
Accepted 17 November 2008
Available online 27 November 2008

OCIS:
300.6450; 170.1530; 170.5660

PACS:
87.64.Je; 87.15.He

Keywords:
Raman spectroscopy
Hepatocyte
Cancer
Doxorubicin

ABSTRACT

Raman spectroscopy has proven to be a very powerful technique and is currently experiencing a renaissance. In this paper, it is used to explore the interaction between doxorubicin and malignant hepatocytes in vitro. For the addition of doxorubicin, the band intensity at 1609 cm^{-1}, mainly assigned to C=C in-plane bending mode of phenylalanine and/or tyrosine residues, increases significantly, and the intensities of the bands at 1585 and 1313 cm^{-1}, mainly due to the guanine bases, decrease greatly. In addition, Raman spectra are investigated at different doxorubicin concentrations, and the mean areas ratios of the band at 1450 to that at 1003 cm^{-1}, A_{1450}/A_{1003}, fluctuate according to the doxorubicin concentration increasing, which suggests that doxorubicin affects the relative content of lipid in cells.

1. Introduction

All diseases and pathological conditions involve biochemical and biophysical intracellular disorders. Monitoring the intracellular disorders and developing is fundamental for understanding various intracellular events, such as cell division, cell differentiation, apoptosis, necrosis, phagocytosis and the interaction of living cells with drugs. The most common and typical methods for probing the morphology and biochemical constitution of cells are electron microscopy, immunocytochemistry, fluorescence spectroscopy, and autoradiography [1,2]. However, these techniques require lengthy procedures (hours, days), large number of cells, and complicated preparations, such as labels or markers, cell lyses and cell fixation.

Raman spectroscopy, based on vibrational spectroscopy, is a rapid and nondestructive technique for studying biological system, e.g. the proteins, nucleic acids, cells and tissues. Raman spectroscopy has the advantages for studying the cells in vitro, namely that no labels and fixation are required. Furthermore, Raman measurements on cells can be performed in physiological-like conditions [3–8]. Since Raman spectrum is sensitive to the chemical and physical changes of biomolecules, it has been successfully used to differentiate the normal and abnormal cells and tissues (cervix, genital tract, brain, breast, larynx, skin and stomach), and investigate the distribution of chemical composition in cells, and measurethe changes at subcellular level induced by the external physical and chemical conditions [9–17]. Besides, Raman spectroscopy has also been widely used to investigate the interaction of the drugs with protein or DNA, and a lot valuable results and information, such as the binding site, the conformational transformation, and the structural change, have been achieved [18–27]. However, the application in antitumor drug interactions with human cells in vitro has not received widespread attention.

Doxorubicin (its molecular structure is shown in Fig. 1) is a kind of antibiotic anticancer drug and has been used for more than 30 years for treating a variety of malignancies. In spite of the extensive clinical utilization of DOX, its mechanism is uncertain. A number of different mechanisms have been proposed, such as intercalation into DNA with the consequent inhibition of macromolecular biosynthesis, free radical formation with the consequent induction of DNA damage or lipid peroxidation, DNA binding and alkylation, DNA cross-linking, interference with DNA unwinding or DNA strand separation and helicase activity, direct membrane effects, and the initiation of DNA damage via the inhibition of topoisomerase [28,29]. In this paper, the interaction between DOX and malignant hepatocytes has been investigated by Raman spectroscopy, and the alteration of intracellular composition and

* Corresponding author. Tel.: +86 21 62232801; fax: +86 21 62232056.
E-mail address: zrsun@phy.ecnu.edu.cn (Z. Sun).

0301-4622/$ – see front matter © 2008 Elsevier B.V. All rights reserved.
doi:10.1016/j.bpc.2008.11.005

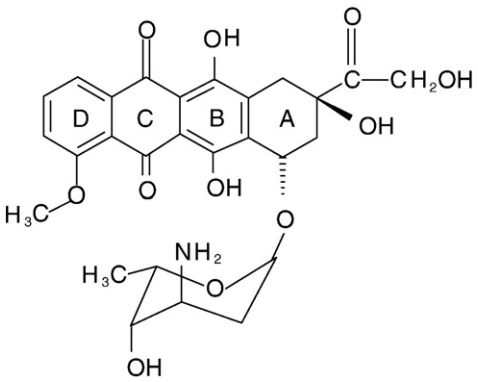

Fig. 1. The chemical structure of DOX.

conformation induced by antitumor drugs has been monitored and the interaction mechanism of DOX with malignant hepatocytes is discussed and analyzed.

2. Materials and methods

2.1. Materials

Cell line BEL-7404 was purchased from the cell bank of Shanghai Institutes for Biological Sciences (Shanghai, China), and fetal calf serums (FCS) and RPMI 1640 medium were purchased from Invitrogen (Carlsbad, CA, USA).

2.2. Cell culture

The cell line of BEL-7404 was cultured in RPMI 1640 with 10% fetal calf serums (Invitrogen, Carlsbad, USA) at 37 °C in a humidified atmosphere containing 5% CO_2. The cells were digested with 0.25% trypsin, resuspended in serum-containing medium to 10^4 cells/mL, and seeded on the quartz slide in culture medium containing DOX for 12 h. Before Raman analysis, the samples were rinsed and immersed in PBS (0.01 M, PH7.2) to remove all growing medium.

2.3. Drug preparation and treatment

The stock solution of DOX was prepared in phosphate-buffered saline (PBS) at the concentration of 0.1 mg/mL. 10, 25, 50, 75, and 100 μL of the stock solution were added into five wells in 24-well chamber, and the final concentrations of DOX were 1.00, 2.50, 5.00, 7.50, and 10.00 μg/mL, respectively.

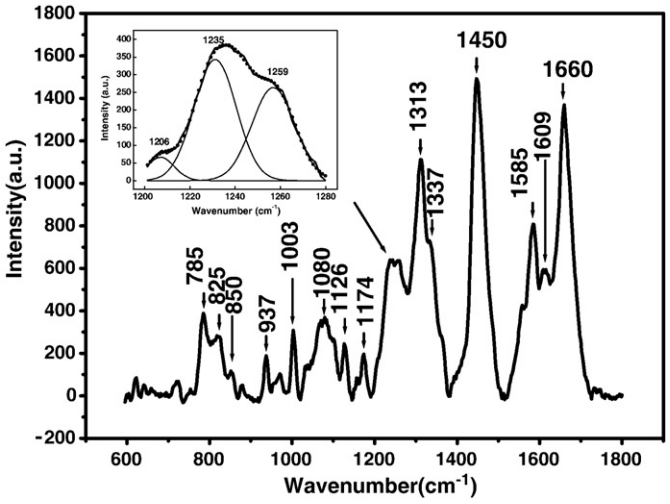

Fig. 2. The mean Raman spectrum of malignant hepatocytes. The inset is the Raman spectrum in the range of 1200–1300 cm^{-1} for AIII of proteins in malignant hepatocytes.

Table 1
Tentative Raman assignments for the malignant hepatocytes

Peak position (cm^{-1})	Assignments			
	Protein	Nucleic acid	Lipid	Ref.
785		C, T, O–P–O		[30,31]
825	Tyr	O–P–O		[30,31]
850	Tyr			[30,31]
937	C–C BK str. α-helix			[30,31]
1003	Phe			[30,31]
1080	C–N str.		C–N str.	[30,31]
1126	.		C–C str.	[30,31]
1174	Tyr			[30,31]
1200–1300	AIII C–N str.			[30,31]
1313		G		[30,31]
1337	CH bend, Trp	A (N7C5, C8N7)		[30,31]
1450			CH_2 def	[30,31]
1585		G (C4N3–C5C4–N7C5), A (C5C4–C4N3)		[20,30,31]
1609	Phe, Tyr			[30,31,32]
1660	AI C=O str.		C=C str.	[30,31]

Abbreviations: A, adenine; G, guanine; C, cytosine; T, thymine; BK, backbone; Phe, phenylalanine; Tyr, tyrosine; Trp, tryptophan; def, deformation; str., stretching.

2.4. Raman spectroscopy

Raman spectra were recorded by a confocal micro-Raman spectrometer (T64000, Jobin-Yvon, France), equipped with a 50 mW argon–krypton laser excitation source at 514 nm, a microscope (IX 81, Olympus, Japan), a holographic notch filter to reject Rayleigh scattering and a liquid nitrogen cooled CCD detector (CCD-3000 V, Edison N.J., USA). The spectrometer was calibrated with the silicon phonon mode at 520 cm^{-1}. A 100× microscope objective (NA 0.95 Olympus), which produced a laser spot size of about 1μm, was used to focus laser and collect Raman scattering on the individual cell. The power at the sample was about 2 mW to ensure no sample degradation occurred. These experimental conditions were kept constant for all measurements. Five cells per sample were analyzed with micro-Raman spectroscopy and three different positions in a cell were measured. The laser beam was interrupted between measurements. Raman spectra in the range of 600–1800 cm^{-1} were recorded with an integration time of 100 s.

2.5. Data treatment

Spectral acquisition and all preliminary spectral correction such as smoothing, baseline subtraction, normalization, and spectral analysis were carried out using the Labspec6.0 software, and the spectra were preprocessed by 5-point smoothing to reduce noise. Raman spectrum baseline was corrected by fitting and subtracting a fifth order polynomial function. The Raman signal of the PBS and the fluorescence background of DOX were subtracted. Each Raman spectrum was normalized using entire spectral range of 600–1800 cm^{-1}.

3. Results and discussion

3.1. Overview of malignant hepatocytes Raman spectra

The mean Raman spectrum of malignant hepatocytes is shown in Fig. 2, and their tentative assignments are also listed in Table 1. As shown in the insert of Fig. 2, the fitting curve in the amide III region reveals the secondary structure of protein in malignant hepatocytes. The major peak at the 1235 cm^{-1} arises from the beta sheet conformation. The peak at 1259 cm^{-1} may arise from the alpha

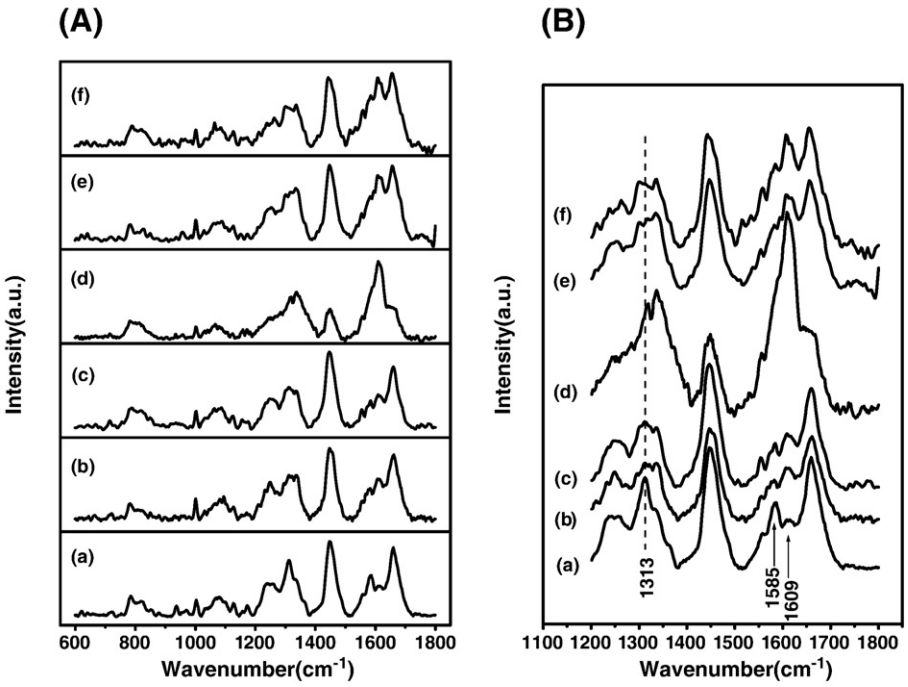

Fig. 3. (A) The mean Raman spectra of DOX treated malignant hepatocytes at the DOX concentrations of 0 (a), 1.00 (b), 2.50 (c), 5.00 (d), 7.50 (e), and 10.00 (f) μg/mL. (B) The magnified Raman spectra in the region of 1100–1800 cm^{-1}.

helical conformation which is confirmed by the presence of the band at 937 cm^{-1} assigned to C–C stretching motions in the protein backbone. The band at 1003 cm^{-1} is the symmetric ring breathing mode of phenylalanine [24,25]. The bands at 825 and 850 cm^{-1} are due to Fermi resonance between the ring breathing vibration and the overtone of an out of plane ring bending vibration of the parasubstituted benzenes of tyrosine. The band at 784 cm^{-1} arises from the overlap of the 782 cm^{-1} and 791 cm^{-1} bands, which can be assigned to cytosine and a stretching vibration of backbone phosphodiester groups of B-form DNA, respectively [33]. So the band at 785 cm^{-1} in Fig. 2 suggests that the conformation of DNA is B-form.

3.2. Impact of DOX on the malignant hepatocytes

Fig. 3(A) shows the Raman spectra arranged from bottom to top with the DOX concentration increasing. Several predominant bands at 1660, 1450, and 1003 cm^{-1} are observed, and there appear significant changes of the spectral profile as the concentration of DOX increasing. Fig. 3(B) shows the dependence of the detailed spectra on the concentrations of DOX in the region of 1100–1800 cm^{-1}. The spectral profile in the region of 1200–1300 cm^{-1} for proteins AIII appear great changes, and results in the alteration of secondary structure of proteins induced by the environmental alterations of amino acids.

The band intensity at 1609 cm^{-1}, assigned to C=C in-plane bending mode of phenylalanine and/or tyrosine residues, increases remarkably, and it is suggested that a vital change in the environment of the Phe and/or Tyr residues of malignant hepatocyte proteins. In the living malignant hepatocyte, the protein folds in an ordered structure and the Phe/Tyr side chain may be "buried" or "masked", and so their Raman intensity appears rather weak [34]. When treated by antitumor drug, DOX, the hydrogen bond will be disrupted, and the Phe/Tyr side chain will be "exposed", and so the exposed Phe/Tyr will generate a large Raman scattering at 1609 cm^{-1}.

The relative intensities of the Raman bands at 830 and 850 cm^{-1} are related to the environment of the tyrosine side chain [35]. If the tyrosine, as a strong hydrogen-bond donor, is buried, the intensity ratio of the band at 850 cm^{-1} to that at 830 cm^{-1}, I_{853}/I_{830}, is about 0.5. As shown in Fig. 2, their intensity ratio, I_{850}/I_{825}, is about 0.43, and it is inferred that tyrosine is buried and phenolic group acts as hydrogen bond donor. As shown in Fig. 3(A), the spectral profile in range of 800–860 cm^{-1} arose changes for DOX addition and the intensity ratio of the band at 850 cm^{-1} to that at 825 cm^{-1}, I_{850}/I_{825}, has slight increase. The experimental result suggests that DOX alters the environment of tyrosine in cells and parts of tyrosine residues are exposed.

As shown in Fig. 3(B), there observed the significant changes in the region of 1100–1800 cm^{-1}. The band at 1585 cm^{-1}, corresponding to the overlap of the C4N3–C5C4–N7C5 vibration mode of guanine (G) and C5C4–C4N3 vibration mode of adenine (A) [20], shows a strong decrease by the addition of DOX, and more the band at 1313 cm^{-1}, assigned to guanine (G), decreases and shifts from 1313 cm^{-1} to 1317 cm^{-1} as DOX increasing. It suggests that DOX may interact with the N7 and/or N3 position of guanine in DNA. As aforementioned, the DNA in malignant hepatocytes is B-form, and guanine is exposed to the major groove. The hydroxylcyclohexylether-amine-group in DOX is similar to a polyamine, and it can bind preferentially in the major groove of B-form DNA [36]. So, it is reasonable that DOX interacts with guanine. As the N7 and N3 positions of guanine are proton–acceptor sites, it is very probable that DOX interacts with guanine via the formation of hydrogen bond with the N7/N3 position of guanine. However, in view of the stereo-hindrance effect, N7 is more reactive than N3, and so DOX will interact with the N7 position of guanine by hydrogen bond.

3.3. Influence of DOX concentrations on malignant hepatocytes

The bands at 1450 and 1003 cm^{-1} can be assigned to lipids and proteins, respectively. Their relative intensity can reveal a structural modification. In order to evaluate the structural alteration induced by

Table 2
The mean area of Raman bands at 1450 and 1003 cm^{-1}, and the ratio of these two bands at different concentration DOX

Concentration of DOX (μg/mL)	0	1.00	2.50	5.00	7.50	10.00
A_{1450}	19.8	19.1	20.2	7.9	18.4	15.8
A_{1003}	1.1	1.2	1.1	0.8	1.1	0.8
A_{1450}/A_{1003}	18.0	15.9	18.4	7.9	16.7	19.7

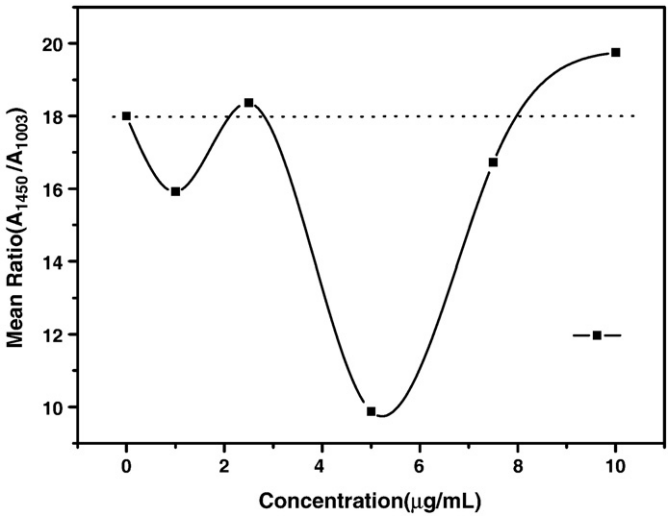

Fig. 4. The mean ratio between the 1450 cm^{-1} and 1003 cm^{-1} bands (A_{1450}/A_{1003}) at different DOX concentration (squares).

DOX, the band mean areas ratio, A_{1450}/A_{1003}, has been calculated for DOX-free and DOX treated cells (as shown in Table 2). As we can see from Fig. 4, the mean ratio fluctuates according to the concentration of DOX. As the concentration of DOX is in the range of 0–2.50 and 7.5–10.0 μg/mL, the fluctuation range is small. As the concentration of DOX increase from 2.50 to 7.50 μg/mL, the fluctuation range increases sharply. The ratio first decreases rapidly and then increases, and the ratio reaches the lowest point at about 5.00 μg/mL. It means that the relative content of lipids in cells will fluctuate according to the change of concentration of DOX. As the concentration of DOX is about 5.00 μg/mL, the influence of DOX on the malignant hepatocytes is the strongest.

4. Conclusions

In this paper, the Raman spectra for the malignant hepatocytes treated by DOX have been explored. The changes in the Raman bands for the guanine (1313 cm^{-1} and 1585 cm^{-1}) of DNA suggest that DOX may interact with DNA by the hydrogen bond to the N7 position of guanine. The antitumor drug, DOX, affects the secondary structure and the environment of the amino acids of protein in malignant hepatocyte, and the Phe/Tyr side chain and tyrosine residue become exposed by the addition of DOX. The area ratio of the band at 1450 cm^{-1} to that at 1003 cm^{-1} will fluctuate according to the concentration of DOX, and it indicates that relative content of lipids in cells is affected by the DOX concentration increasing.

Acknowledgements

This research was supported by National Natural Science Foundation of China (No. 10574046), National Key Project for Basic Research of China (No. 2006CB806006 and 2006CB921105), Supported by Program for Changjiang Scholars and Innovative Research Team in University (PCSIRT), Programme for New Century Excellent Talents in University (NCET-04-0420), the Doctoral Programme of High Education (No. 20050269011), Phosphor Programme sponsored by Shanghai Science and Technology Committee (No. 06QH14003). Z. R. Sun is the correspondence author, and his e-mail is zrsun@phy.ecnu.edu.cn

References

[1] C. Kraff, T. Knetschke, A. Siegner, R.H.W. Funk, R. Salzer, Mapping of single cells by near infrared Raman microspectroscopy, Vib. Spectrosc. 32 (2003) 75–83.
[2] N. Uzunbajakava, A. Lenferink, Y. Kraan, E. Volokhina, G. Vrensen, J. Greve, C. Otto, Nonresonant confocal Raman imaging of DNA and protein distribution in apoptotic cells, Biophys. J. 84 (2003) 3968–3981.
[3] R. Malini, K. Venkata Krishna, J. Kurien, M. Pai Keerthilatha, Rao Lakshmi, V.B. Karatha, C. Murali Krishna, Discrimination of normal, inflammatory, premalignant, and malignant oral tissue: a Raman spectroscopy study, Biopolymers 81 (2006) 179–193.
[4] B. Schrader, B. Dippel, I. Erb, S. Keller, T. Löchte, H. Schulz, E. Tatsch, S. Wessel, NIR Raman spectroscopy in medicine and biology: results and aspects, J. Mol. Struct. 480–481 (1999) 21–32.
[5] I. Notingher, G. Jell, P.L. Notingher, I. Bisson, O. Tsigkou, J.M. Polak, M.M. Stevens, L. Hench, Multivariate analysis of Raman spectra for in vitro non-invasive studies of living cells, J. Mol. Struct. 744–747 (2005) 179–185.
[6] H.P. Buschman, G. Deinum, J.T. Motz, M. Fitzmaurice, J.R. Kramer, A. Van der Laarse, A.V. Bruschke, M.S. Feld, Raman microspectroscopy of human coronary atherosclerosis: biochemical assessment of cellular and extracellular morphologic structure in situ, Cardiovasc. Pathol. 10 (2000) 69–82.
[7] I. Notingher, I. Bisson, J.M. Polak, L.L. Hench, In situ spectroscopic study of nucleic acids in differentiating embryonic stem cells, Vib. Spectrosc. 35 (2004) 199–203.
[8] Y. Takai, T. Masuko, H. Takeuchi, Lipid structure of cytotoxic granules in living human killer T lymphocytes studied by Raman microspectroscopy, Biochim. Biophys. Acta 1335 (1997) 199–208.
[9] C.M. Krishna, G.D. Sockalingum, B.M. Vadhiraja, K. Maheedhar, A.C.K. Rao, L. Rao, L. Venteo, M. Pluot, D.J. Fernandes, M.S. Vidyasagar, V.B. Kartha, M. Manfait, Vibrational spectroscopy studies of formalin-fixed cervix tissues, Biopolymers 85 (2007) 214–221.
[10] P. Crow, A. Molckovsky, N. Stone, J. Uff, B. Wilson, L.M. Wongkeesong, Assessment of fiberoptic near-infrared Raman spectroscopy for diagnosis of bladder and prostate cancer, Urology 65 (2005) 1126–1130.
[11] N. Stone, C. Kendall, N. Shepherd, P. Crow, H. Barr, Near-infrared Raman spectroscopy for the classification of epithelial pre-cancer and cancers, J. Raman Spectrosc. 33 (2002) 564–573.
[12] Z.W. Huang, A.M. Williams, H. Liu, Near-infrared Raman spectroscopy for optical diagnosis of lung cancer, Int. J. Cancer 107 (2003) 1047–1052.
[13] R. Manoharan, Y. Wang, M.S. Feld, Histochemical analysis of biological tissues using Raman spectroscopy, Spectrochim. Acta A 52 (1996) 215–249.
[14] C. Krafft, T. Knetschke, R.H.W. Funk, R. Salzer, Studies on stress-induced changes at subcellular level by Raman microspectroscopic mapping, Anal. Chem. 78 (13) (2006) 4424–4429.
[15] J. Choi, J. Choo, H. Chung, D.G. Gweon, J. Park, H.J. Kim, S. Park, C.H. Oh, Direct observation of spectral differences between normal and basal cell carcinoma tissues using confocal Raman microscopy, Biopolymers 77 (2005) 264–272.
[16] S. Fendel, B. Schrader, Investigation of skin and skin lesions by NIR-FT-Raman spectroscopy, Fresenius J. Anal. Chem. 360 (1998) 609–613.
[17] A.V. Feofanov, A.I. Grichine, L.A. Shitova, T.A. Karmakova, R.I. Yakubovskaya, M. Egret-Charlier, P. Vigny, Confocal Raman microspectroscopy and imaging study of theraphthal in living cancer cells, Biophys. J. 78 (2000) 499–512.
[18] C. Ortiz, D. Zhang, A.E. Rigge, Y. Xie, D. Ben-Amotz, Analysis of insulin amyloid fibrils by Raman spectroscopy, Biophys. Chem. 128 (2007) 150–155.
[19] A. Sukhanova, S. Grokhovsky, M. Ermishov, K. Mochalov, A. Zhuze, V. Oleinikov, I. Nabiev, DNA structural alterations induced by bis-netropsins modulate human DNA topoisomerase I cleavage activity and poisoning by camptothecin, Biochem. Pharmacol. 64 (2002) 79–90.
[20] J. Stanicová, G. Fabriciová, L. Chinsky, V. Šutiak, P. Miškovský, Amantadine–DNA interaction as studied by classical and resonance Raman spectroscopy, J. Mol. Struct. 478 (1999) 129–138.
[21] J.M. Benevides, G. Chan, X.J. Lu, W.K. Olson, M.A. Weiss, G.J. Thomas, Protein-directed DNA structure. I. Raman spectroscopy of a high-mobility-group box with application to human sex reversal, Biochemistry 39 (2000) 537–547.
[22] C.I. Morari, C.M. Muntean, Numerical simulations of Raman spectra of guanine–cytosine Watson-crick and protonated hoogsteen base pairs, Biopolymers 72 (2003) 339–344.
[23] R.T. Forbes, B.W. Barry, A.A. Elkordy, Preparation and characterisation of spray-dried and crystallised trypsin: FT-Raman study to detect protein denaturation after thermal stress, Eur. J. Pharm. Sci. 30 (2007) 315–323.
[24] F. Fleury, A. Ianoul, M. Berjot, A. Feofanov, A.J.P. Alix, I. Nabiev, Camptothecin-binding site in human serum albumin and protein transformations induced by drug binding, FEBS Lett. 411 (1997) 215–220.
[25] J.V. Tattini, D.F. Parra, B. Polakiewicz, R.N.M. Pitombo, Effect of lyophilization on the structure and phase changes of PEGylated-bovine serum albumin, Int. J. Pharm. 304 (2005) 124–134.
[26] N.K. Afseth, J.P. Wold, V.H. Segtnan, The potential of Raman spectroscopy for characterisation of the fatty acid unsaturation of salmon, Anal. Chim. Acta 572 (2006) 85–92.
[27] K. Nakamura, S. Era, Y. Ozaki, M. Sogami, T. Hayashi, M. Murakami, Conformational changes in seventeen cystine disulfide bridges of bovine serum albumin proved by Raman spectroscopy, FEBS Lett. 17 (1997) 375–378.
[28] D.A. Gewirtz, A critical evaluation of the mechanisms of action proposed for the antitumor effects of the anthracycline antibiotics adriamycin and daunorubicin, Biochem. Pharmacol. 57 (1999) 727–741.
[29] Q. Yan, W. Priebe, J.B. Chaires, R.S. Czernuszewicz, Interaction of doxorubicin and its derivatives with DNA: elucidation by resonance Raman and surface-enhanced resonance Raman spectroscopy, Biospectroscopy 3 (1997) 307–316.
[30] I. Notingher, S. Verrier, S. Haque, J.M. Polak, L.L. Hench, Spectroscopic study of human lung epithelial cells (A549) in culture: living cells versus dead cells, Biopolymers 72 (2003) 230–240.
[31] I. Notingher, J. Selvakumaran, L.L. Hench, New detection system for toxic agents based on continuous spectroscopic monitoring of living cells, Biosens. Bioelectron. 20 (2004) 780–789.

[32] I. Notingher, G. Jell, U. Lohbauer, V. Salih, L.L. Hench, In situ non-invasive spectral discrimination between bone cell phenotypes used in tissue engineering, J. Cell. Biochem. 92 (2004) 1180–1192.
[33] O. Vrána, V. Mašek, V. Dražan, V. Brabec, Raman spectroscopy of DNA modified by intrastrand cross-links of antitumor cisplatin, J. Struct. Biol. 159 (2007) 1–8.
[34] C. Xie, C. Goodman, M. Dinno, Y.Q. Li, Real-time Raman spectroscopy of optically trapped living cells and organelles, Opt. Express 12 (2004) 6208.
[35] Y. Xie, D. Zhang, G.K. Jarori, V.J. Davisson, D. Ben-Amotza, The Raman detection of peptide tyrosine phosphorylation, Anal. Biochem. 332 (2004) 116–121.
[36] L.B. Liao, H.Y. Zhou, X.M. Xiao, Spectroscopic and viscosity study of doxorubicin interaction with DNA, J. Mol. Struct. 749 (2005) 108–113.